A 2-fold interpenetrating 3D pillar-layered MOF for gas separation and detection of metal ions

Guoqiang Peng,[a] Zhibo, Su,[a] Falu Hu,*[a] Zhenyu Ji,[b] Zhengyi Di,[c] Guihua Li,[a] Tingting Gao,[a] Guowei Zhou,*[a] Mingyan Wu,*[b]

[a] Key Laboratory of Fine Chemicals in Universities of Shandong, Jinan Engineering Laboratory for Multi-scale Functional Materials, School of Chemistry and Chemical Engineering, Qilu University of Technology (Shandong Academy of Sciences), Jinan 250353, P. R. China

[b] State Key Laboratory of Structure Chemistry, Fujian Institute of Research on the Structure of Matter, Chinese Academy of Sciences, Fuzhou, 350002, P. R. China

[c] Tianjin Key Laboratory of Structure and Performance for Functional Molecules, College of Chemistry, Tianjin Normal University, Tianjin 300387, P. R. China

Email: faluhu@qlu.edu.cn; gwzhou@qlu.edu.cn; wumy@fjirsm.ac.cn.

Experimental section

Materials and methods

All reagents and solvents used in synthesis are commercially available and used as supplied without further purification. Single crystal X-ray diffraction experiments were performed on a Bruker D8-Venture diffractometer equipped with a Cu microfocus tube (λ = 1.54178 Å). Powder X-ray diffraction (PXRD) analyses were carried out on a Rigaku Ultima-IV unit using Cu Ka radiation (λ = 1.54178 Å). Thermogravimetric analyses were recorded on a Q5000IR unit at a heating rate of 10 ^{o}C min^{-1} under nitrogen atmosphere. Photoluminescence spectra were collected using a FLS920 spectrometer with 450 W xenon light. The mass spectra were measured on the ultra high resolution time of flight mass spectrometry (UHR-TOF). Gas sorption isotherms of activated **1a** were measured on a 3-Flex unit. The breakthrough experiments for mixed gas C_2H_6 / CH_4 and CO_2 / N_2 (15±0.5:85±0.5) are carried out at a flow rate of 2 ml / min (298 K, 1 bar) through using a home-built setup coupled with a GC-9860-5CNJ. Activated **1a** powder (43.1 mm and 206 mg) is packed into stainless-steel column ϕ 3 X 180 mm in glove box. Before the breakthrough experiments, the correction factors of C_2H_6 / CH_4 and CO_2 / N_2 (15±0.5:85±0.5) are first performed, respectively. And the binary mixture gas with a flow rate of 2 ml / min (298 K, 1 bar) is introduced through the bypass line with a resistance. And the sample is activated at 80 ^{o}C with 20 ml / min He flow for 10 h. Then the C_2H_6 / CH_4 and CO_2 / N_2 binary mixture gas is first stabilized by flowing through the alternative vent line for 30 min before introducing it as a step input to the adsorption column, respectively.

Synthesis of 4,4',4'',4'''-(thiophene-2,3,4,5-tetrayl)tetrakis(2-fluorobenzoic acid) (H_4tbca-4F). perbromothiophene (6 mmol, 2.4g), ethyl 2-fluoro-4-(4,4,5,5-tetramethyl-1,3,2-dioxaborolan-2-yl)benzoate (28.8 mmol, 8.48 g), cesium carbonate (16.14 g, 50 mol) and tetrakis(triphenylphosphine)palladium (0.4 g, 0. 35 mmol) were

added to a 250 mL Schleck flask charged with stir bar. The flask was pumped under vacuum and refilled with N_2 for three times, and then 150 mL of degassed solvent of 1,4-dioxane was transferred to the system. The solution was heated at 90 °C for 72 h under N_2 atmosphere. After the reaction mixture was cooled to room temperature, the organic solvent was evaporated. The aqueous layer was extracted with dichloromethane (3 × 50 mL) and then the combined organic layers were dried over anhydrous magnesium sulfate and filtered. After removing dichloromethane, the crude product was purified by column chromatography on silica gel to give a yellow solid, which was then dissolved in 100 mL of THF, to which 50 mL of 6 M NaOH aqueous solution was added. The mixture was stirred under reflux for 10 h, before the solvent was removed using a rotary evaporator. The yellow solid was dissolved in water and was acidified with 6 M HCl to yield yellow precipitate of H_4tbca-4F, which was filtered, washed with water, and dried in an oven at 80 °C for 10 h. Yield: 2.4 g, 63 %. ^{1}H NMR (400 MHz, DMSO-d_6): δ, 13.39 (s, 4H), 7.83 (s, 2H), 7.75 (s, 2H), 7.15 (s, 4H), 7.04 (d, 2H), 6.98 (d, 2H).

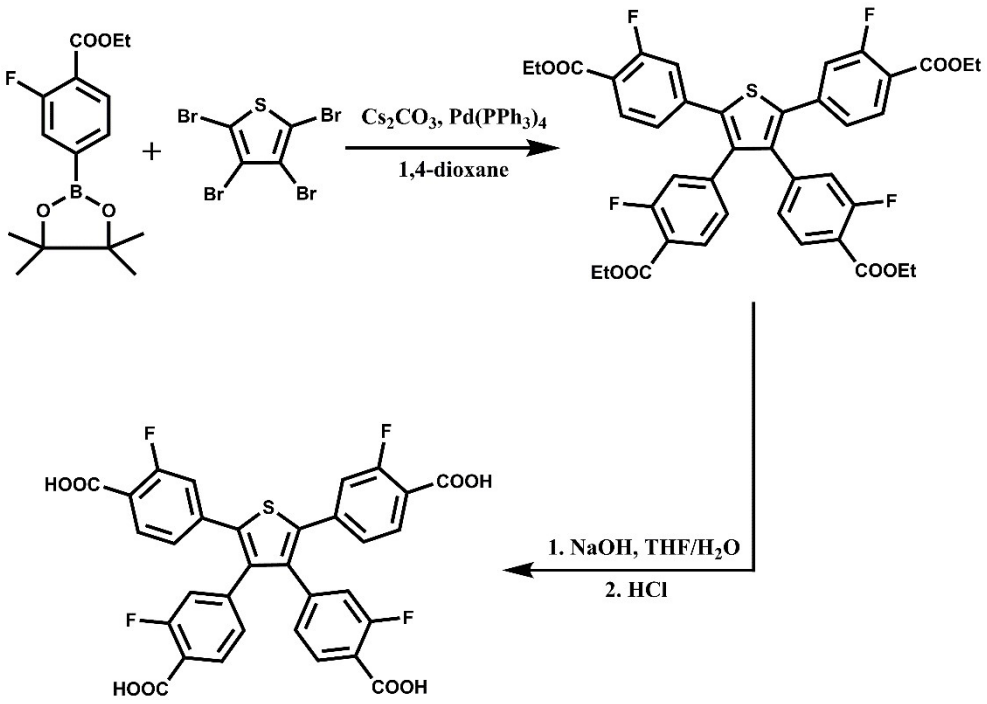

Scheme S1 Synthesis of the H_4tbca-4F ligand

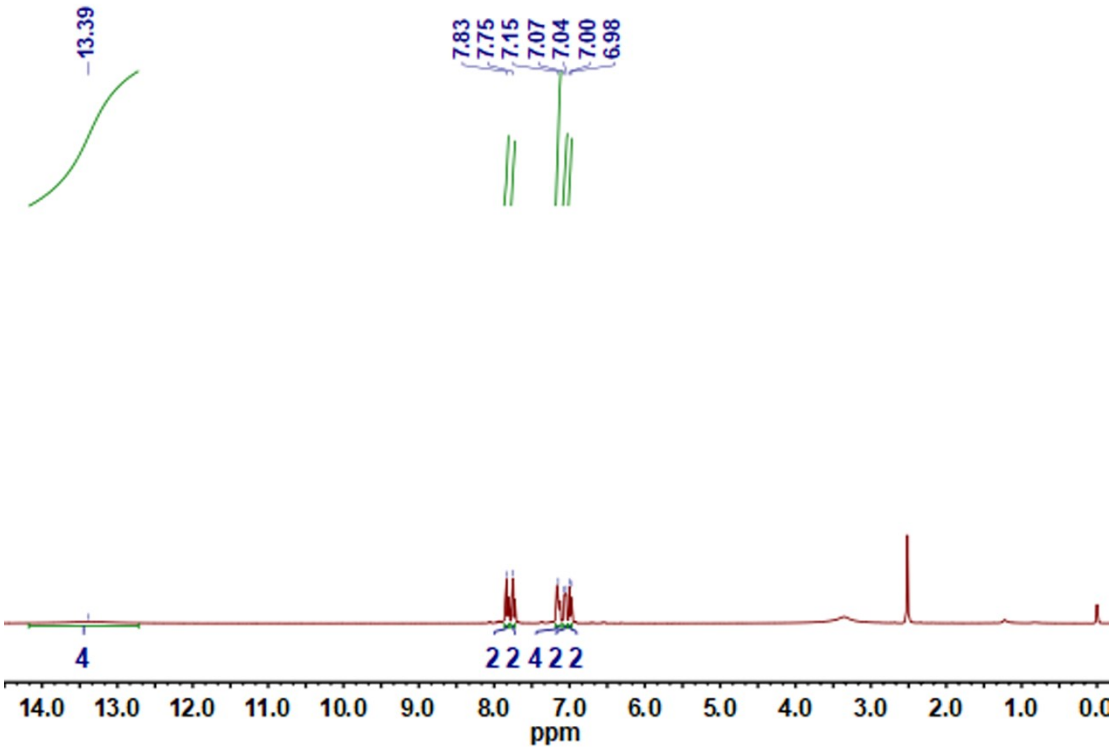

Scheme S2 The NMR spectra of the H_4tbca-4F ligand

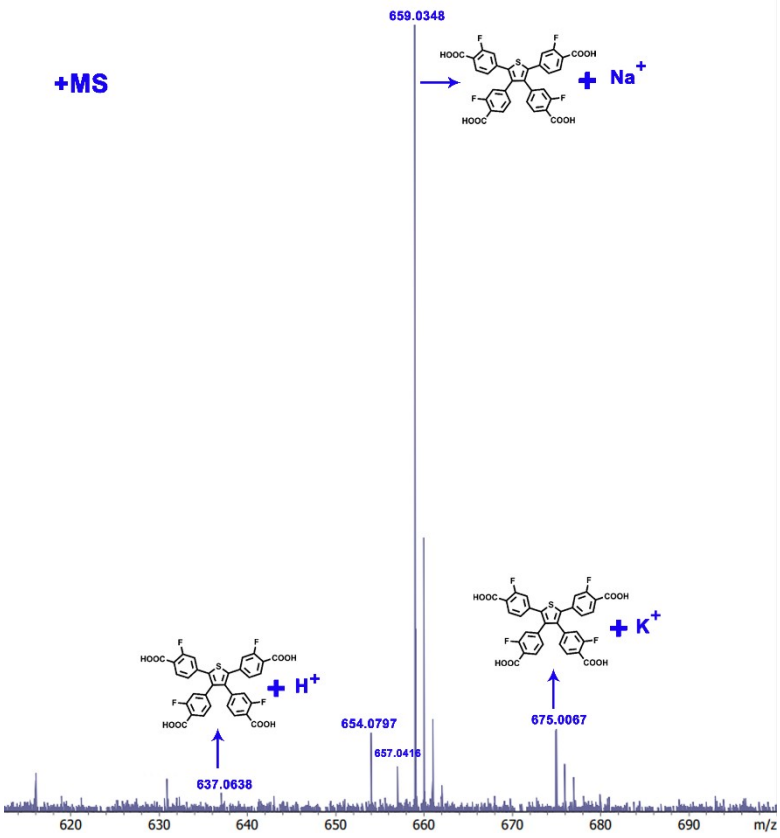

Scheme S3 The ESI-MS of H_4tbca-4F.

Synthesis of Zn_2(tbca-4F)(4,4'-bipyridine)·solvent (1)

$Zn(NO_3)_2·6H_2O$ (30 mg), H_4tbca-4F (7 mg) and 4,4'-bipyridine (5 mg) in the mixture solvents of DMF (1ml), H_2O (0.33ml) and EtOH (0.33ml) in presence of 30 ul HNO_3 were charged in a Pyrex vial at 100 °C for 2 days. Yellow crystals were collected after the reaction (Yield: 53% based on the H_4tbca-4F ligand).

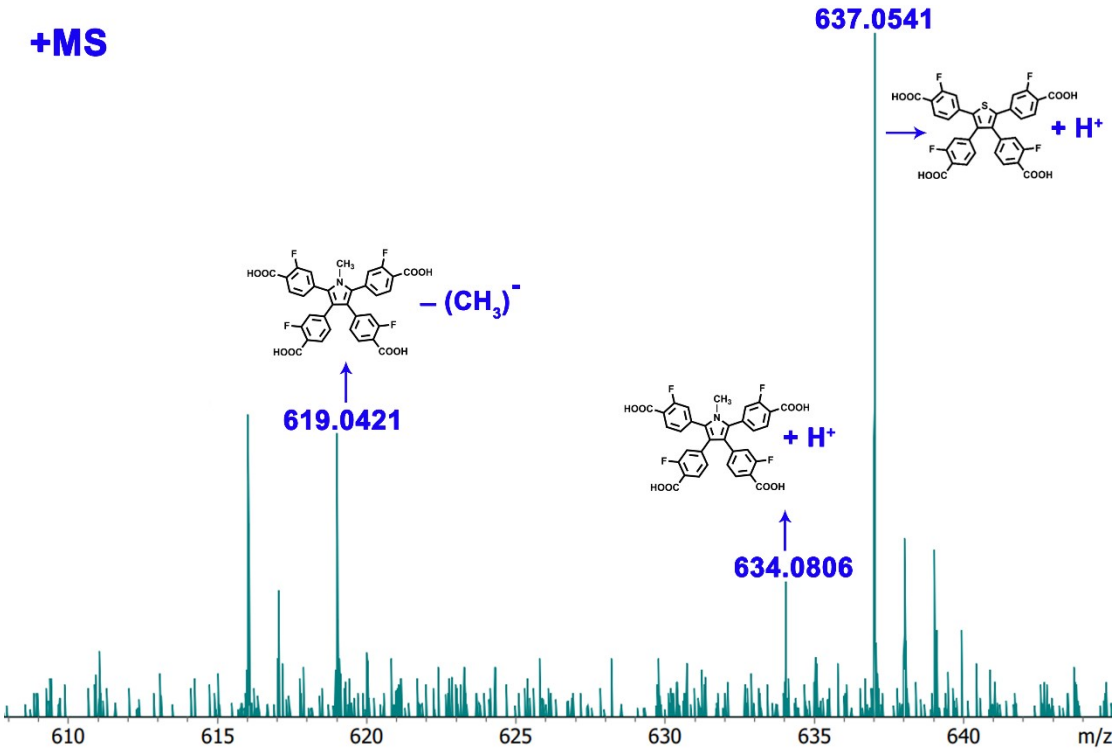

Scheme S4 The ESI-MS of H_4mpca-4F and H_4tbca-4F from the digested **1a** solution.

The IAST Selectivity Calculations

The ideal adsorbed solution theory (IAST) is used to predict the selectivity of binary C_2H_6 / CH_4 and CO_2 / N_2 (15:85) based on single-component adsorption data fitting using the dual-site Langmuir Freundlich (DSLF) equation.

$$N = A_1 \frac{b_1 P^{c_1}}{1 + b_1 P^{c_1}} + A_2 \frac{b_2 P^{c_2}}{1 + b_2 P^{c_2}}$$

p: the pressure of the bulk gas at equilibrium with the adsorbed phase (kPa),

N: the equilibrium adsorbed amount of the adsorbate in an adsorbent (mmol/g),

A_1 and A_2: the saturation uptakes on site 1 and site 2 (mmol/g),

b_1 and b_2: the affinity coefficients of site 1 and site 2 (kPa^{-1}),

c_1 and c_2: the deviations from ideal homogeneous surfaces.

The adsorption selectivities, *S*, for binary mixtures C_2H_6 / CH_4 and CO_2 / N_2 (15:85).

$$S = \frac{x_1/x_2}{y_1/y_2}$$

S: adsorption selectivity

x_i: the mole fractions of component in the adsorbed i (i = 1, 2)

y_i: the mole fractions of component in the bulk phases i (i = 1, 2)

Calculation of isosteric heats of adsorption

We test the adsorption isotherms of C_2H_6, CH_4, CO_2 and N_2 from low pressure to 1 bar at 298 K and 273 K, respectively. And then we used the equation (1) to fit the 298 K and 273 K data. Finally, we used the equation (2) to calculate the isosteric heats of adsorption according to the fitting parameters.

$$\ln P = \ln N + \left(\frac{1}{T}\right)\sum_{i=0}^{m} a_i \times N^i + \sum_{j=0}^{n} b_j \times N^j \qquad (1)$$

P : pressure (mmHg),

N : the amount adsorbed (mg/g),

T : temperature (K),

a_i and b_j: parameters

R: the universal gas constant (8.314 J · mol^{-1} · K^{-1})

m and n determine the number of terms required to adequately describe the isotherm

The isosteric heat of adsorption is calculated according to:

$$Q_{st} = -R \times \sum_{i=0}^{m} a_i \times N^i \qquad (2)$$

Figures

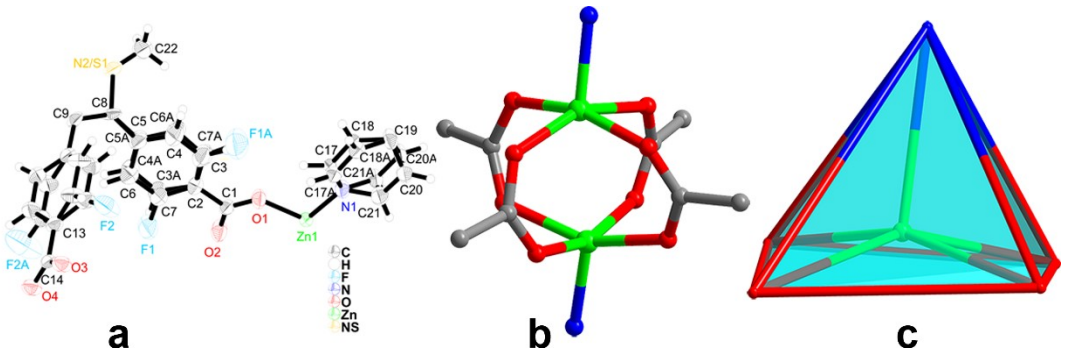

Fig. S1. (a) The asymmetric unit of **1**, S1: Occu: 0.73339; N2: Occu: 0.26661**.** (b) The $Zn_2(COO)_4N_2$ unit of **1**. (c) The geometry of tetragonal pyramid

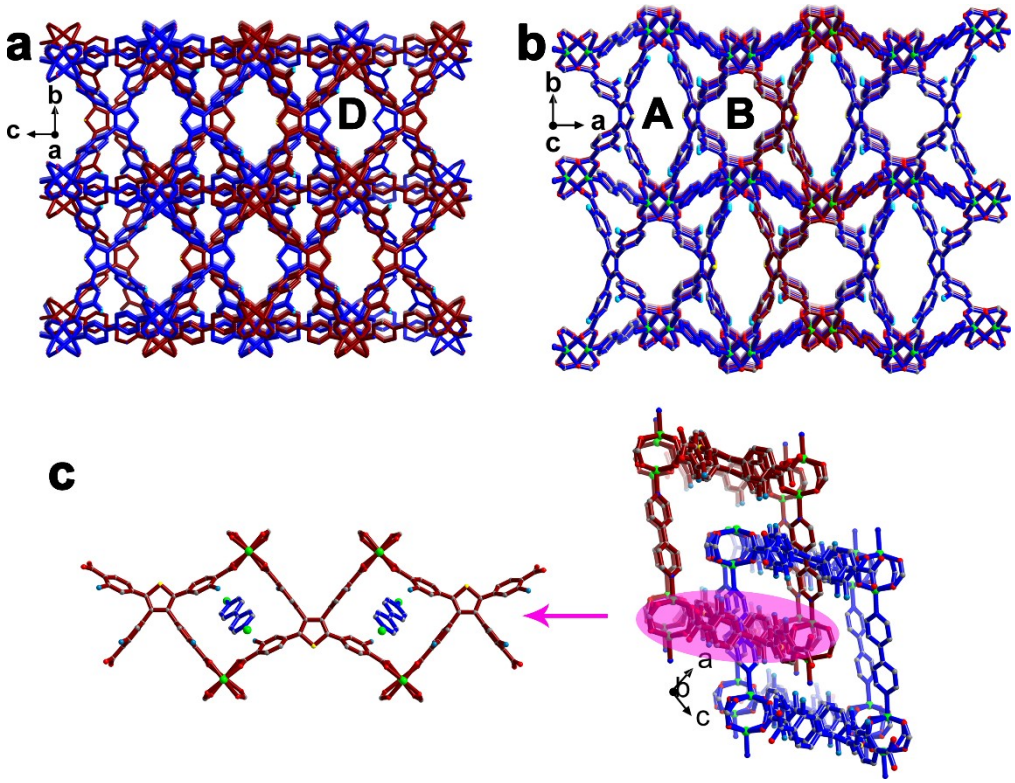

Fig. S2. (a) View of the 2-fold structure along *a* direction. (b) View of the 2-fold structure along *c* direction. (c) The 4,4′-bipyridine linkers interpenetrating the square windows C and the channel of single net.

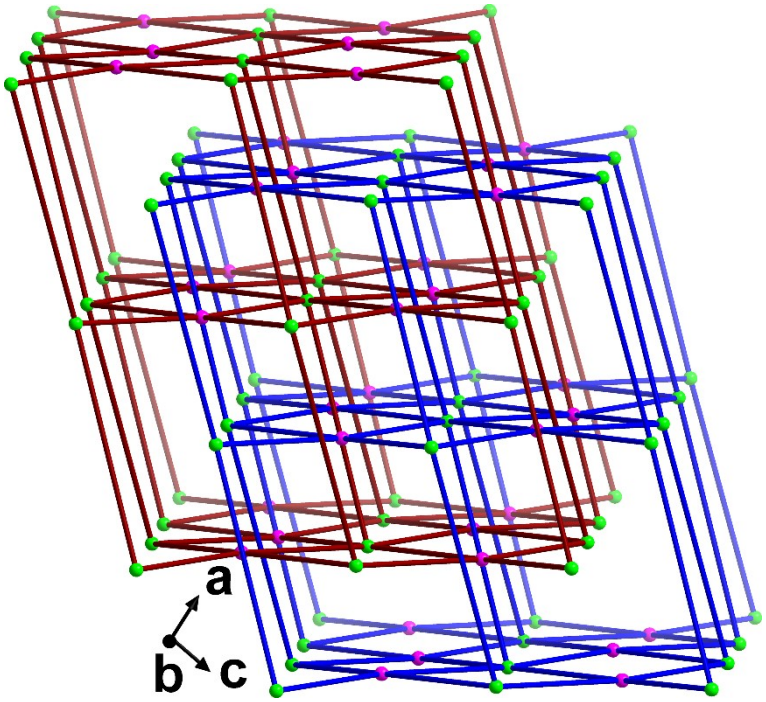

Fig. S3. The ***fsc***-topology of compound **1**

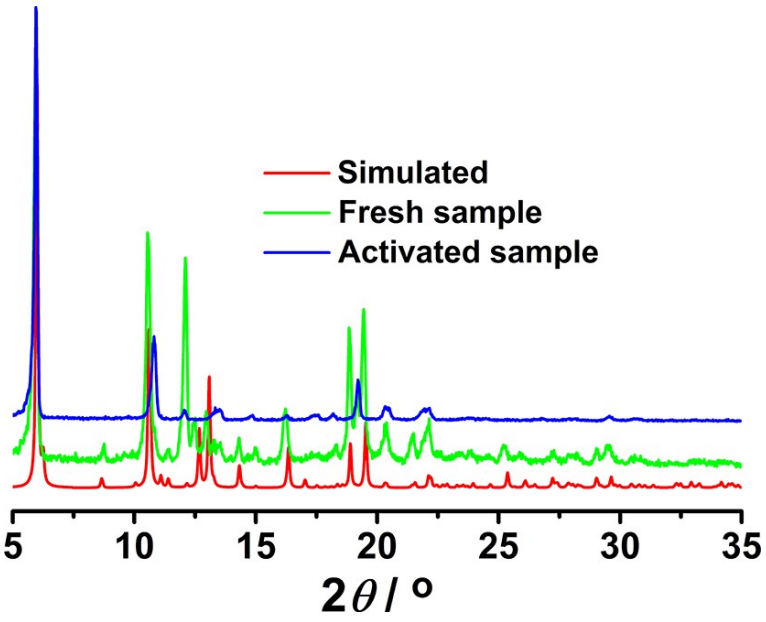

Fig. S4. The PXRD of simulated, fresh and activated sample.

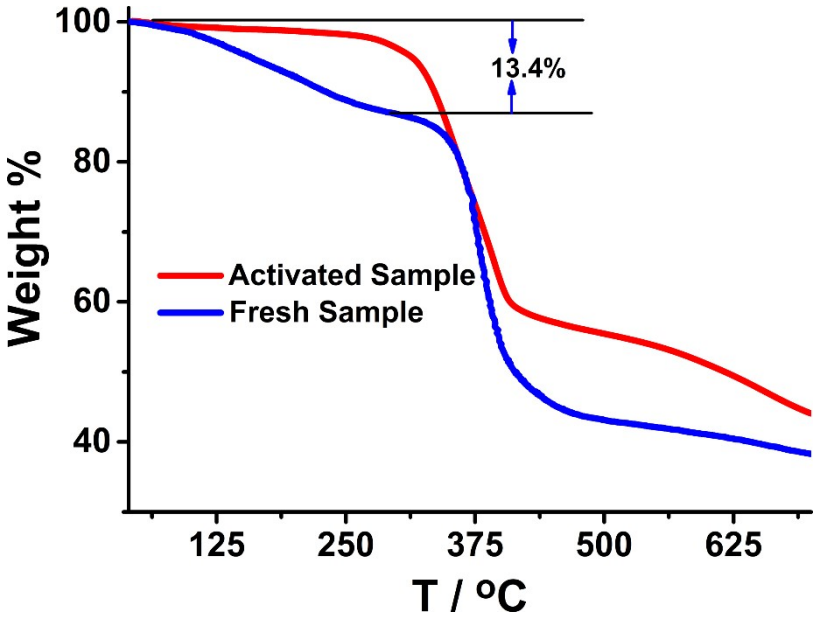

Fig. S5. The TGA curves of fresh sample and activated sample.

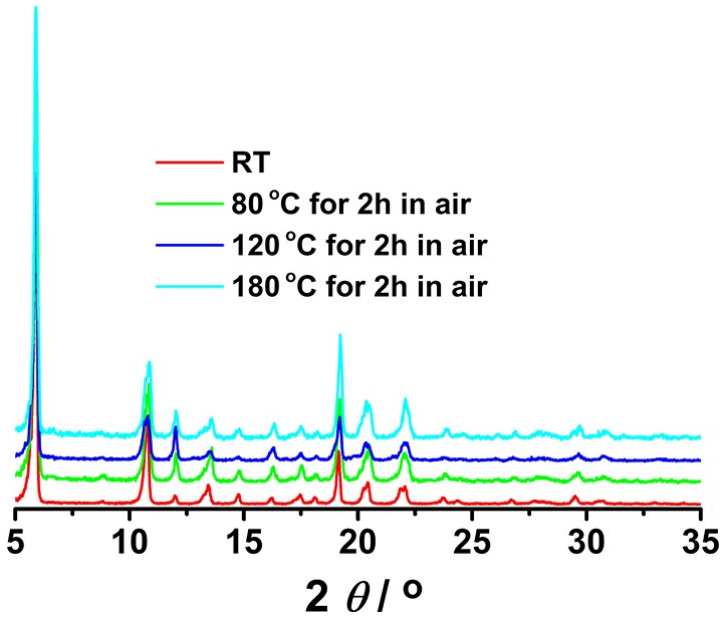

Fig. S6. The variable-temperature PXRD of activated sample

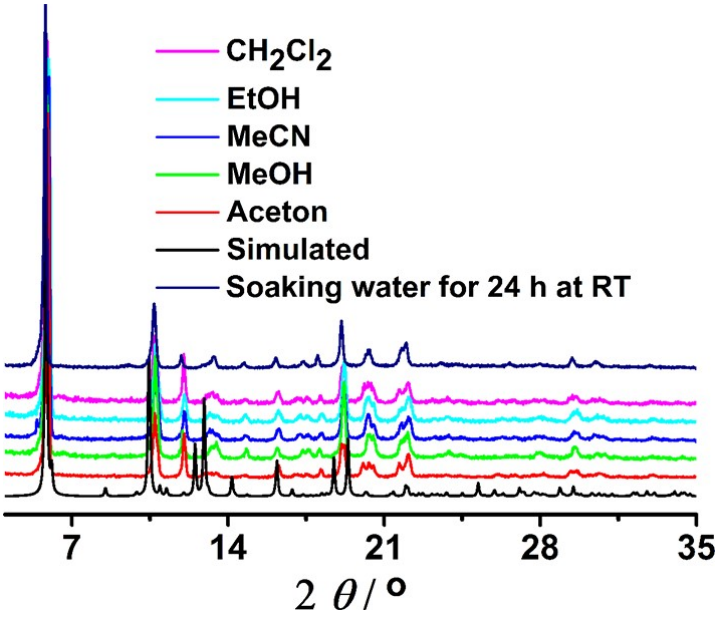

Fig. S7. The PXRD of activated sample soaking in various solvents and water for 24 h

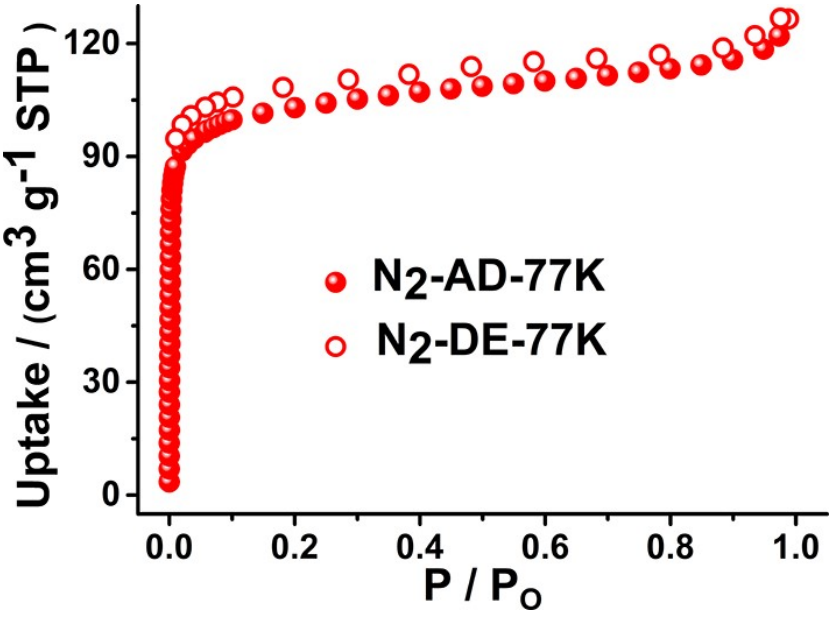

Fig. S8. The N_2 adsorption isotherm at 77 K and 1 bar

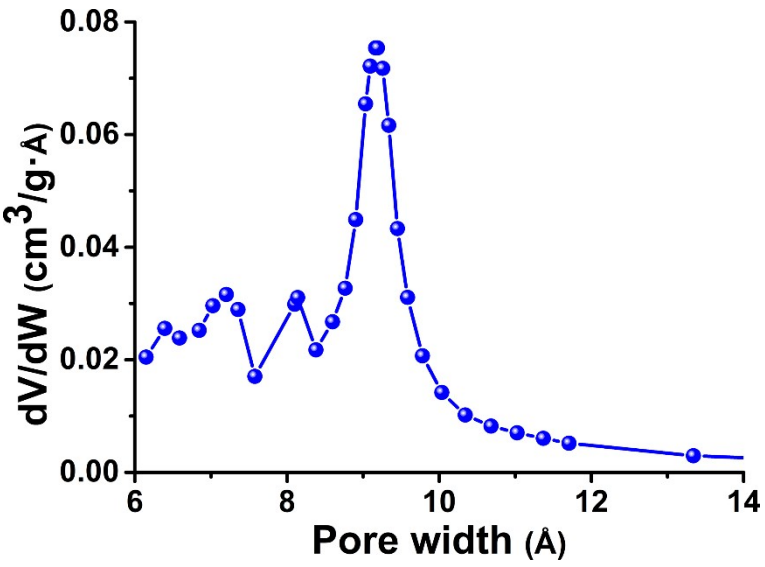

Fig S9 the pore size distribution of **1a**

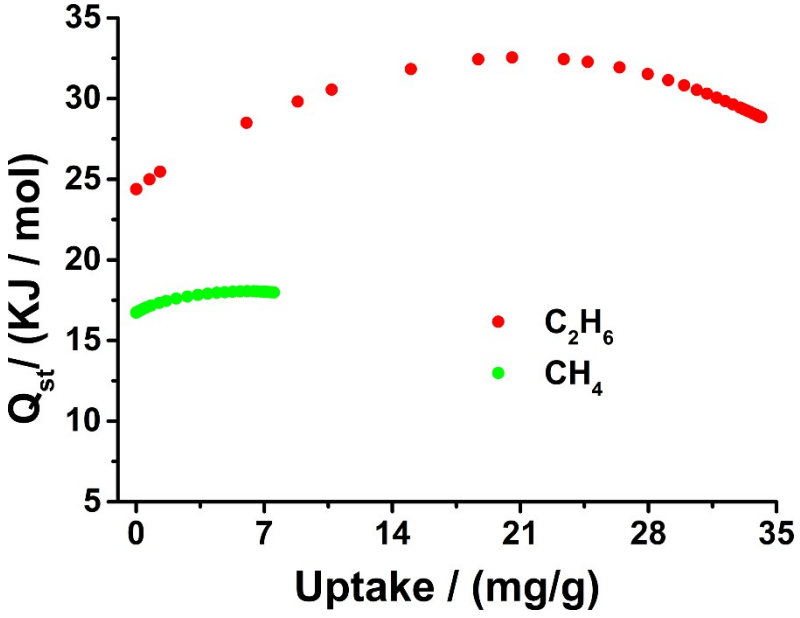

Fig. S10. The isosteric heats of adsorption for C_2H_6 and CH_4 in **1a**

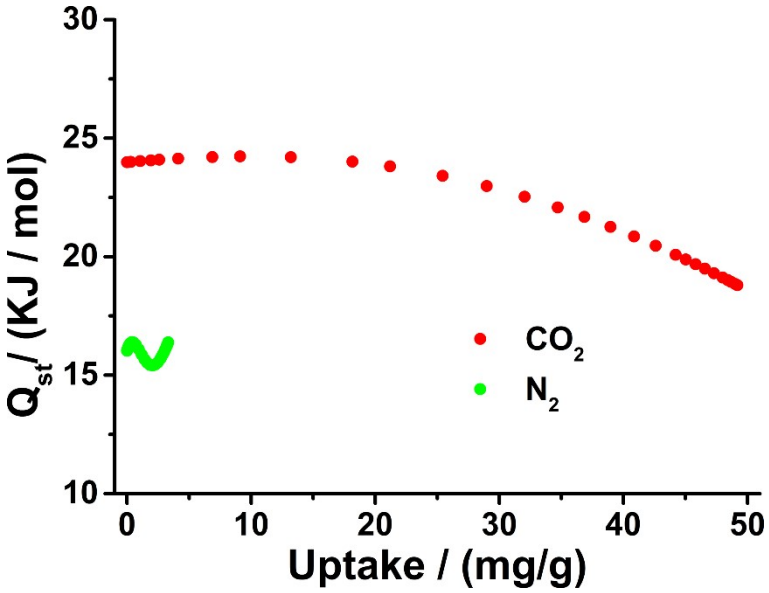

Fig. S11. The isosteric heats of adsorption for CO_2 and N_2 in **1a**

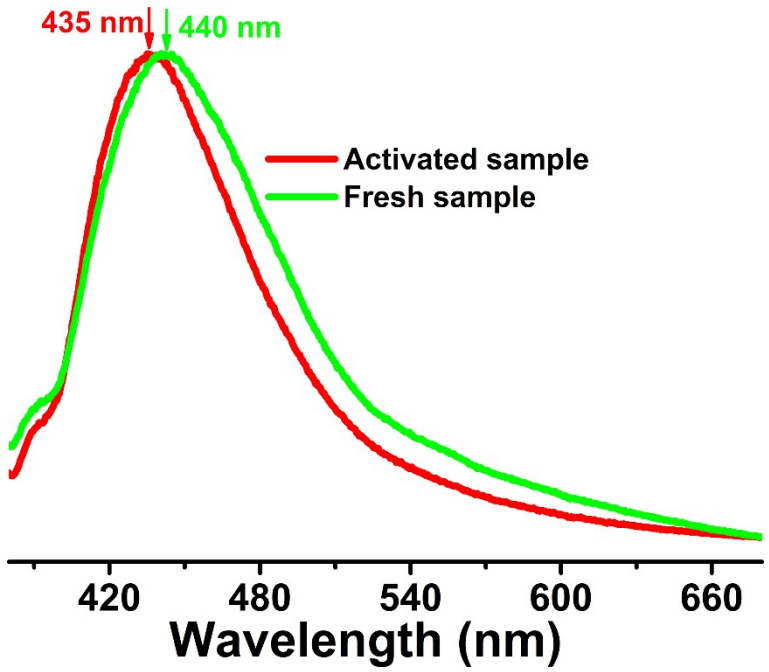

Fig. S12. The solid photoluminescence spectra of activated and fresh samples under 365-excitation nm at room temperature.

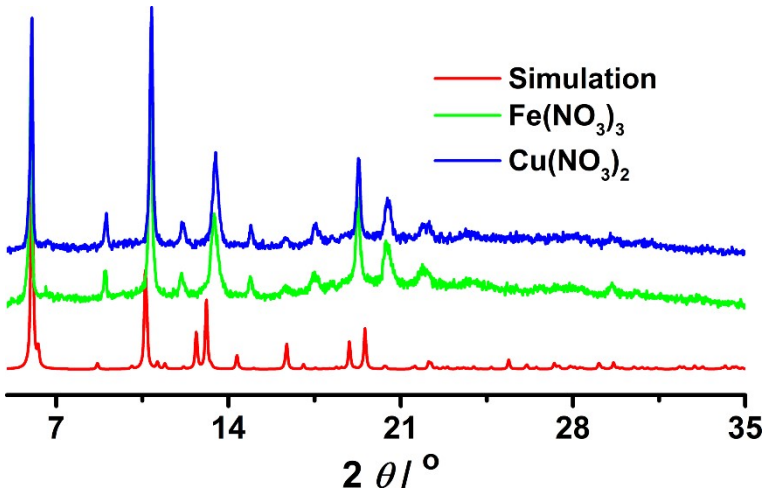

Fig. S13. PXRD patterns of **1a** after soaking in Cu^{2+} and Fe^{3+} aqueous solutions.

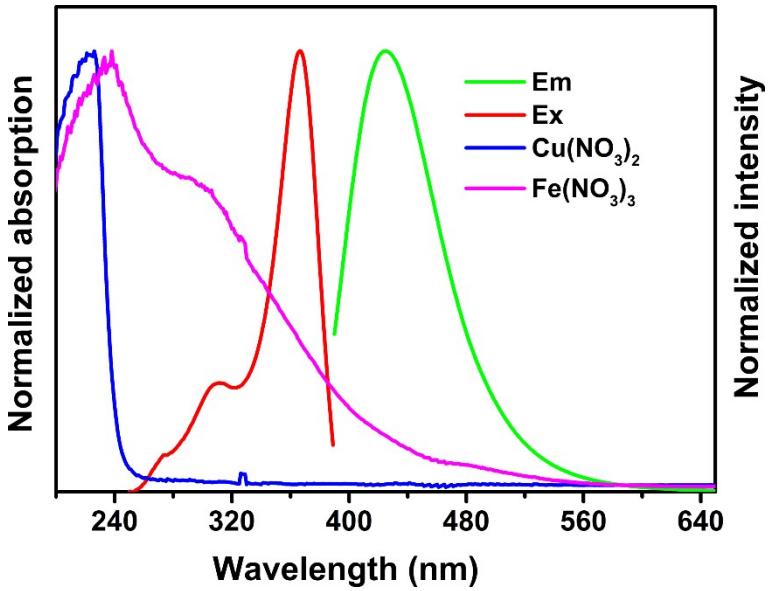

Fig. S14. The UV–vis absorption spectra of the aqueous solutions of Cu^{2+} and Fe^{3+}, and the excitation and emission spectrum of **1a**.

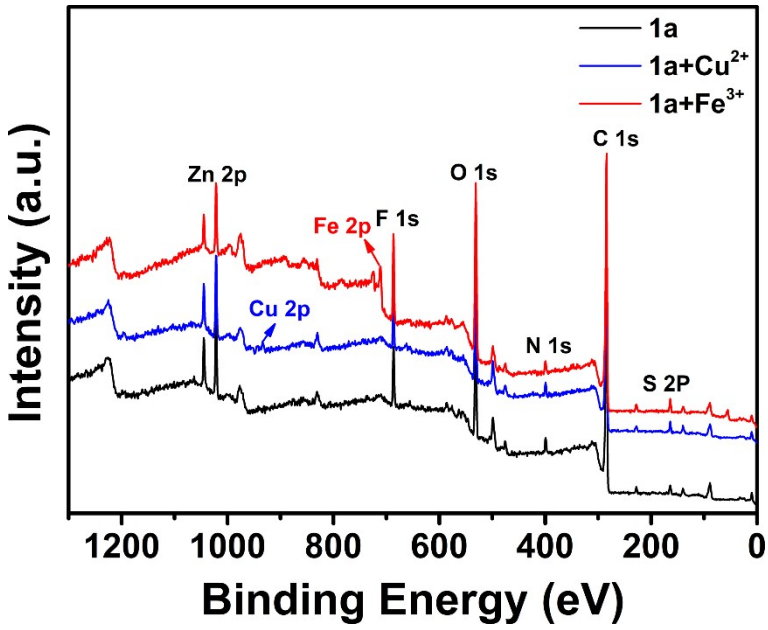

Fig. S15 XPS spectrum of **1a**, Cu^{2+} and Fe^{3+} treated **1a**.

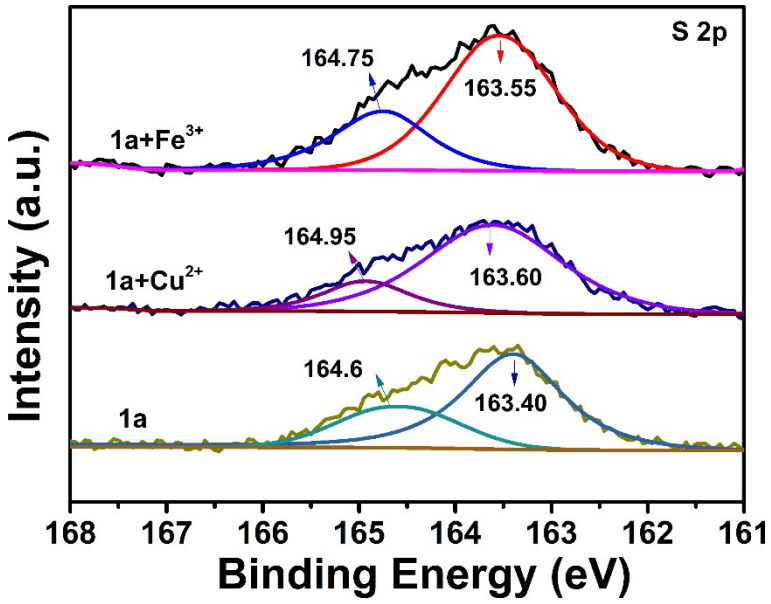

Fig. S16 The high-resolution XPS spectrum for S 2p of **1a**, Cu^{2+} and Fe^{3+} treated **1a**.

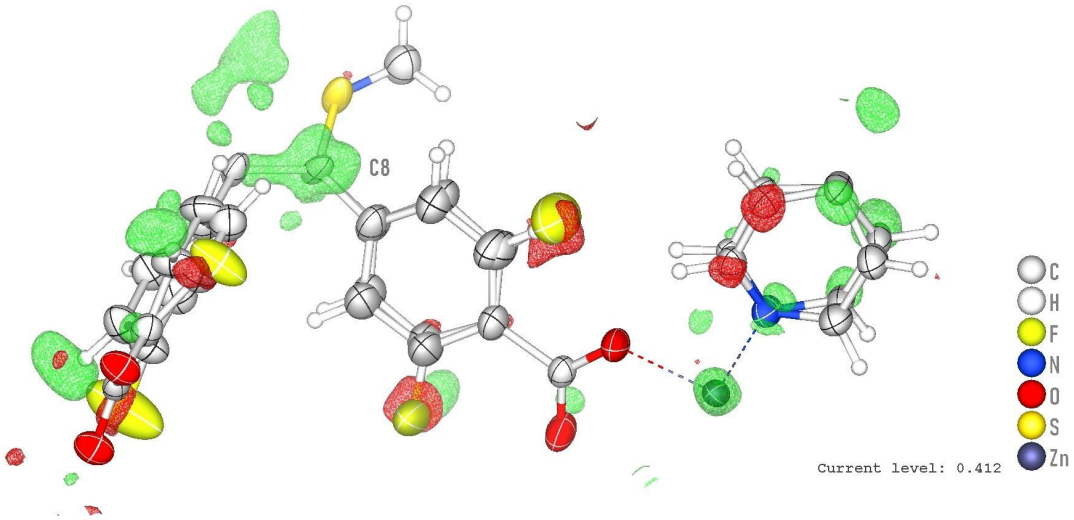

Fig. S17 The residual density plot of asymmetric unit for **1**.

1. Please examine the attached residual density plot. There are problems here; for example, there are more disorde positions for F atoms. It may not be possible and/or necessary to model these -- but the presence of this disorder should be noted.

Response: Thank you for your comment. The disorder positions of F atoms can be addressed with multi-component disorder. Since there are no alert level A and B after checking the structure, we didn't deal with the disorder F atoms.

2. More worryingly, Atom C8 refines quite well as a nitrogen atom -- not enough density has been modelled here. Please check this very carefully. If you still think that this structure is correct, please add the attached images to the SI and discuss the concerns that I have made in this review.

Response: Thank you for pointing this out. After checking carefully, we think the structure is correct. Based on the mass spectrometry data of the original ligand and digest **1a** (Scheme S3 and Scheme S4), we found that only H_4tbca-4F or H_4mpca-4F ligand is present, while neither 4,4',4",4"'-(1,2,5-thiadiazole-2,3,4,5-tetrayl)tetrakis(2-fluorobenzoic acid) nor 4,4',4",4"'-(2-methyl-1H-1,2,3-triazole-1,3,4,5(2*H*)-tetrayl)tetrakis(2-fluorobenzoic acid) ligand is observed. In addition, atom C8 is located on the five-membered heterocycle, which can increase the electron cloud density of the carbon atoms because of the electronic delocalization effect, so the identified atom C8 does not have enough electron cloud density in this position. Thus, we think this structure is correct.

Tables

Table S1. Important crystal data of compound **1** (CCDC number: 2369823)

Identification code	**1**	
Empirical formula	$C_{21.13}H_{10.40}F_2N_{1.13}O_4S_{0.37}Zn,1[C_3H_7NO]$	
Formula weight	532.39	
Temperature	110.0 (2)	
Wavelength	1.54184 Å	
Crystal system	monoclinic	
Space group	*C*2/*m*	
Unit cell dimensions	a = 15.8989(6) Å	α=γ= 90º
	b = 28.7314(10) Å	β= 98.472(2)º
	c = 10.1425(4) Å	
Volume	4582.5(3) $Å^3$	
Z	8	
Density (calculated)	1.331 g/cm^3	
Absorption coefficient	2.169 mm^{-1}	
F(000)	1848.0	
Theta range for data collection	3.076 to 72.530	
Completeness to theta = 67.684	98%	
Crystal size	0.13 × 0.12 × 0.11 mm^3	
Data/restraints/parameters	4561/509/413	
Goodness-of-fit on F^2	1.053	
Final R indices [I>2sigma(I)]	R_1 = 0.0701, wR_2 = 0.2000	
R indices (all data)	R_1 = 0.0861, wR_2 = 0.2190	
Largest diff. peak and hole	1.17/-0.68 e.$Å^{-3}$	

Table S2. Bond lengths [Å] and angles [°] of compound **1**.			
Zn(1)-O(1)	1.999(3)	O(1)-Zn(1)-O(3)#6	160.64(15)
Zn(1)-O(3)#4	2.000(3)	O(1)-Zn(1)-N(1)	96.93(15)
Zn(1)-N(1)	2.034(4)	O(3)#6-Zn(1)-N(1)	101.53(15)
Zn(1)-O(4)#5	2.053(3)	O(1)-Zn(1)-O(4)#5	89.54(16)
Zn(1)-O(2)#3	2.114(4)	O(3)#6-Zn(1)-O(4)#5	88.53(15)
		N(1)-Zn(1)-O(4)#5	113.15(16)
		O(1)-Zn(1)-O(2)#3	87.06(17)
		O(3)#6-Zn(1)-O(2)#3	86.41(17)
		N(1)-Zn(1)-O(2)#3	92.41(16)
		O(4)#5-Zn(1)-O(2)#3	154.44(14)
		O(1)-Zn(1)-Zn(1)#3	82.78(10)
		O(3)#6-Zn(1)-Zn(1)#3	77.92(10)
		N(1)-Zn(1)-Zn(1)#3	166.94(13)
		O(4)#5-Zn(1)-Zn(1)#3	79.92(10)
		O(2)#3-Zn(1)-Zn(1)#3	74.53(10)

Symmetry transformations used to generate equivalent atoms:

#3 2-X,+Y,1-Z; #4 -1/2+X,1/2-Y,-1+Z; #5 3/2-X,1/2-Y,-Z; #6 1/2+X,1/2-Y,1+Z.

Table S3. Comparison of gas separation of porous adsorbents for C_2H_6 over CH_4	
Compound	C_2H_6/CH_4
[1]DMOF-$(CF_3)_2$	~15
[2]MIL-126(Fe/Co)	13.2
[3]MOF-303	26
[4]JUC-220	46
[5]CFA-1-$NiCl_2$-2.3	15.2
[6]SNNU-Bai78	40
[7]LIFM-W2	19
[8]HOF-ZJU-201a	45
[8]HOF-ZJU-202a	36
[9]Ni(HBTC)(bipy)	27.5
[10]Ni-BPZ	67.6
[11]Ni(TMBDC)$(DABCO)_{0.5}$	29
[12]$Zn_9(tba)_9(dabco)_3$	16
[13]BSF-1	23
[14]BSF-2	53
[15]NbU-5	27.2

[16]SBMOF-1	74
[16]SBMOF-2	26
[17]JLU-Liu18	13.1
[18]FJI-C1	9
[19]UTSA-35a	15
[20]JLU-Liu46	17
[21]GNU-1a	17.5
[22]DMOF-Cl	12.5
[23]ZnBPZ-SA	10.9
[24]Fe-pyz	23
[25]Ni(4-DPDS)$_2$CrO$_4$	33.9
This work	77.6

Table S4. Comparison of gas separation of porous adsorbents for CO_2 over N_2.	
Compound	CO_2/N_2
[26]HBU-23	28.4
[27][Zn$_2$(tdc)$_2$dabco]	11.2
[28]Eu-MOF	28.7
[29]ROD-7	23
[29]ROD-6	15 to 17
[29]NU-1000	9
[30]BUT-10	18.6
[30]BUT-11	31.5
[30]UiO-67	9.4
[31]TMU-34(−2H)	29.5
[32]ZJNU-40	22.9
[33]MOC-QW-3-NH$_2$	23
[34]SIFSIX-2-Cu	13.5
[35]ZIF-300	22
[36]LIFM-10	18.3
[37]MOF-5	9
[38]PCN-88	15.2
[39]NOTT-202	26.7
[40]NbO-Pd-1	33.5
[41]PCN-222	32.5
[42]MW-140	31
[43]NJU-Bai50	30.5
[44]UPC-70	32
This work	34

References

1. L. Yan, H. T. Zheng, L. Song, Z. W. Wei, J. J. Jiang and C. Y. Su, *ACS Appl. Mater. Interfaces*, 2024, **16**, 6579-6588.
2. Y. Wang, X. Zhao, S. Han and Y. Wang, *ACS Appl. Mater. Interfaces*, 2024, **16**, 10468-10474.
3. S. Xian, J. Peng, H. Pandey, T. Thonhauser, H. Wang and J. Li, *Engineering*, 2023, **23**, 56-63.
4. X. Shi, Y. Zu, X. Li, T. Zhao, H. Ren and F. Sun, *Nano Research*, 2023, **16**, 10652-10659.
5. J. Peng, J. Zhong, Z. Liu, H. Xi, J. Yan, F. Xu, X. Chen, X. Wang, D. Lv and Z. Li, *ACS Appl. Mater. Interfaces*, 2023, **15**, 41466-41475.

6. H. Cheng, Q. Wang and J. Bai, *Chem. Eur. J.*, 2023, **29**, e202202047.
7. W. Wang, X. H. Xiong, N. X. Zhu, Z. Zeng, Z. W. Wei, M. Pan, D. Fenske, J. J. Jiang and C. Y. Su, *Angew. Chem. Int. Ed.*, 2022, **61**, e202201766.
8. Y. Liu, Q. Xu, L. Chen, C. Song, Q. Yang, Z. Zhang, D. Lu, Y. Yang, Q. Ren and Z. Bao, *Nano Research*, 2022, **15**, 7695-7702.
9. P. Guo, M. Chang, T. Yan, Y. Li and D. Liu, *Chin. J. Chem. Eng.*, 2022, **42**, 10-16.
10. S. Tu, L. Yu, D. Lin, Y. Chen, Y. Wu, X. Zhou, Z. Li and Q. Xia, *ACS Appl. Mater. Interfaces*, 2022, **14**, 4242-4250.
11. Y. Wu, Z. Liu, J. Peng, X. Wang, X. Zhou and Z. Li, *ACS Appl. Mater. Interfaces*, 2020, **12**, 51499-51505.
12. D. Wang, X. Dong, Y. Han and Y. Liu, *Nano Research*, 2020, **14**, 526-531.
13. Y. Zhang, L. Yang, L. Wang, S. Duttwyler and H. Xing, *Angew. Chem. Int. Ed.*, 2019, **58**, 8145-8150.
14. Y. Zhang, L. Yang, L. Wang, X. Cui and H. Xing, *Journal of Materials Chemistry A*, 2019, **7**, 27560-27566.
15. J. Li, S. Chen, L. Jiang, D. Wu and Y. Li, *Inorg. Chem.*, 2019, **58**, 5410-5413.
16. A. M. Plonka, X. Chen, H. Wang, R. Krishna, X. Dong, D. Banerjee, W. R. Woerner, Y. Han, J. Li and J. B. Parise, *Chem. Mater.*, 2016, **28**, 1636-1646.
17. S. Yao, D. Wang, Y. Cao, G. Li, Q. Huo and Y. Liu, *J. Mater. Chem. A*, 2015, **3**, 16627-16632.
18. Y. Huang, Z. Lin, H. Fu, F. Wang, M. Shen, X. Wang and R. Cao, *ChemSusChem*, 2014, **7**, 2647-2653.
19. Y. He, Z. Zhang, S. Xiang, F. R. Fronczek, R. Krishna and B. Chen, *Chem. Commun.*, 2012, **48**, 6493-6495.
20. B. Liu, S. Yao, X. Liu, X. Li, R. Krishna, G. Li, Q. Huo and Y. Liu, *ACS Appl. Mater. Interfaces*, 2017, **9**, 32820-32828.
21. S. M. Li, H. C. Jiang, Q. L. Ni, L. C. Gui and X. J. Wang, *Dalton Trans*, 2023, **52**, 9655-9663.
22. Z. Song, Y. Zheng, Y. Chen, Y. Cai, R. J. Wei and J. Gao, *Dalton Trans*, 2023, **52**, 15462-15466.
23. G.-D. Wang, R. Krishna, Y.-Z. Li, Y.-Y. Ma, L. Hou, Y.-Y. Wang and Z. Zhu, *ACS Materials Letters*, 2023, **5**, 1091-1099.

24. L. Zhao, P. Liu, C. Deng, T. Wang, S. Wang, Y.-J. Tian, J.-S. Zou, X.-C. Wu, Y. Zhang, Y.-L. Peng, Z. Zhang and M. J. Zaworotko, *Nano Research*, 2023, **16**, 12338-12344.
25. F. Zheng, R. Chen, Z. Zhang, Q. Yang, Y. Yang, Q. Ren and Z. Bao, *Cell Rep. Phys. Sci*, 2022, **3**, 100903.
26. S.-Q. Gang, Z.-Y. Liu, Y.-N. Bian, R. Wang and J.-L. Du, *Sep. Purif. Technol.*, 2024, **335**, 126153.
27. V. A. Bolotov, K. A. Kovalenko, D. G. Samsonenko, X. Han, X. Zhang, G. L. Smith, L. J. McOrmick, S. J. Teat, S. Yang, M. J. Lennox, A. Henley, E. Besley, V. P. Fedin, D. N. Dybtsev and M. Schröder, *Inorg. Chem.*, 2018, **57**, 5074-5082.
28. W.-M. Liao, M.-J. Wei, J.-T. Mo, P.-Y. Fu, Y.-N. Fan, M. Pan and C.-Y. Su, *Dalton Trans.*, 2019, **48**, 4489-4494.
29. R. J. Li, M. Li, X. P. Zhou, D. Li and M. O'Keeffe, *Chem. Commun.*, 2014, **50**, 4047-4049.
30. B. Wang, H. Huang, X. L. Lv, Y. Xie, M. Li and J. R. Li, *Inorg. Chem.*, 2014, **53**, 9254-9259.
31. S. A. Razavi, M. Y. Masoomi, T. Islamoglu, A. Morsali, Y. Xu, J. T. Hupp, O. K. Farha, J. Wang and P. C. Junk, *Inorg. Chem.*, 2017, **56**, 2581-2588.
32. C. Song, Y. He, B. Li, Y. Ling, H. Wang, Y. Feng, R. Krishna and B. Chen, *Chem. Commun.*, 2014, **50**, 12105-12108.
33. L.-Z. Qin, X.-H. Xiong, S.-H. Wang, L.-L. Meng, T.-A. Yan, J. Chen, N.-X. Zhu, D.-H. Liu and Z.-W. Wei, *Inorg. Chem.*, 2021, **60**, 17440-17444.
34. P. Nugent, Y. Belmabkhout, S. D. Burd, A. J. Cairns, R. Luebke, K. Forrest, T. Pham, S. Ma, B. Space, L. Wojtas, M. Eddaoudi and M. J. Zaworotko, *Nature*, 2013, **495**, 80-84.
35. N. T. Nguyen, H. Furukawa, F. Gandara, H. T. Nguyen, K. E. Cordova and O. M. Yaghi, *Angew. Chem. Int. Ed.*, 2014, **53**, 10645-10648.
36. Y. Xiong, Y. Z. Fan, R. Yang, S. Chen, M. Pan, J. J. Jiang and C. Y. Su, *Chem. Commun.*, 2014, **50**, 14631-14634.
37. N. Ding, H. Li, X. Feng, Q. Wang, S. Wang, L. Ma, J. Zhou and B. Wang, *J. Am. Chem. Soc.*, 2016, **138**, 10100-10103.
38. J. R. Li, J. Yu, W. Lu, L. B. Sun, J. Sculley, P. B. Balbuena and H. C. Zhou, *Nat. Commun.*, 2013, **4**, 1538.
39. S. Yang, X. Lin, W. Lewis, M. Suyetin, E. Bichoutskaia, J. E. Parker, C. C. Tang, D. R. Allan,

P. J. Rizkallah, P. Hubberstey, N. R. Champness, K. M. Thomas, A. J. Blake and M. Schroder, *Nat Mater*, 2012, **11**, 710-716.

40. I. Spanopoulos, I. Bratsos, C. Tampaxis, D. Vourloumis, E. Klontzas, G. E. Froudakis, G. Charalambopoulou, T. A. Steriotis and P. N. Trikalitis, *Chem. Commun.*, 2016, **52**, 10559-10562.
41. D. Lv, R. Shi, Y. Chen, Y. Chen, H. Wu, X. Zhou, H. Xi, Z. Li and Q. Xia, *Ind. Eng. Chem. Res.*, 2018, **57**, 12215-12224.
42. C. Chen, X. Feng, Q. Zhu, R. Dong, R. Yang, Y. Cheng and C. He, *Inorg. Chem.*, 2019, **58**, 2717-2728.
43. X. Song, M. Zhang, J. Duan and J. Bai, *Chem. Commun.*, 2019, **55**, 3477-3480.
44. X. Wang, Y. Wang, K. Lu, W. Jiang and F. Dai, *Chin. Chem. Lett.*, 2021, **32**, 1169-1172.